F-15 Nozzle/Afterbody Integration

Richard E. Martens*
McDonnell Aircraft Company, St. Louis, Mo.

The performance of the F-15 represents a significant improvement over that of current operational fighter aircraft. A major contributor in attaining this improvement was the efficient integration of the engine and nozzle with the airframe. This integration was accomplished experimentally because the nozzle/afterbody flowfield is too complex for theoretical evaluation. During the F-15 development program, both two-dimensional and axisymmetric nozzle installations were considered. The selected nozzle/afterbody configuration is characterized by close-spaced, axisymmetric C-D nozzles installed in a carefully contoured afterbody with wide-spaced tail support booms. The considerations leading to the selection and performance substantiation of the F-15 nozzle/afterbody configuration are reviewed in this paper.

Nomenclature

A_{ex}	= nozzle exit area
A_{max}	= fuselage maximum cross-sectional area
A_t	= nozzle throat area
C_D	= aerodynamic drag coefficient, $D/q\ S_w$ (friction plus pressure drag unless noted)
$C_{D,P}$	= aerodynamic pressure drag coefficient, D/qS_w
C_P	= surface pressure coefficient, $(P_\ell - P_0)/q$
$F_{g_{ideal}}$	= nozzle ideal gross thrust for complete isentropic expansion of actual jet flow to ambient static pressure
$F_{g_{rev}}$	= nozzle gross thrust with reverser deployed (in drag direction)
M_0	= freestream Mach number
P_{ex}	= nozzle exit static pressure
P_0	= ambient static pressure
P_ℓ	= local static pressure
P_{T_J}/P_0	= nozzle pressure ratio (nozzle jet total pressure/ambient static pressure)
P_s	= specific excess power
q	= freestream dynamic pressure
R_e	= Reynolds number based on total fuselage length
S_w	= aircraft reference wing area (608 ft^2)
S/D_{eng}	= distance between engines/maximum engine diameter (also maximum nozzle diameter)
TOGW	= aircraft takeoff gross weight
α	= aircraft angle of attack
β	= local flow angle

Introduction

THE performance of the F-15 represents a significant improvement over that of current operational fighter aircraft. A major contributor to this improvement was the efficient integration of the engine and nozzle with the airframe. Nozzle/airframe integration has become a major consideration in the design of advanced fighter aircraft because the nozzle cross-sectional area accounts for as much as 55% of the maximum fuselage cross-sectional area. Furthermore, the variation in geometry of the nozzle between cruise and afterburning power introduces changes in projected area which can increase the drag coefficient up to $\Delta C_D = 0.0060$.

Presented as Paper 74-1100 at the AIAA/SAE 10th Propulsion Conference, San Diego, Calif., Oct. 21-23, 1974; submitted Jan. 6, 1975; revision received Aug. 1, 1975.

Index categories: Aircraft Configuration Design; Aircraft Performance; Aircraft Testing (including Component Wind Tunnel Testing).

*Section Manager, Propulsion. Member AIAA.

The F-15 integration was accomplished experimentally since the interactions of the jet with the external flowfield are too complex for theoretical evaluation. However, the test data available at the start of the F-15 program were too limited to develop an efficient nozzle/afterbody design. Consequently, a configuration development program was conducted, which consisted of both static and wind-tunnel testing, to support extensive engine/airframe trade studies. A performance verification program was subsequently accomplished in the wind tunnel to refine the basic design and predict aircraft performance. The objective of this paper is to review the considerations leading to the selection and performance substantiation of the F-15 nozzle/afterbody configuration.

Nozzle/Afterbody Configuration Development

Extensive system design studies and parallel test programs were conducted in the development of the F-15 nozzle/afterbody. This effort involved both conventional axisymmetric and two-dimensional (2-D) nozzle installations. The important elements of these multi-discipline trade studies and test programs which led to the selection of the final configuration are described in the following paragraphs.

Axisymmetric Nozzle/Afterbody

Installation of axisymmetric nozzles in twin-engine fighter aircraft introduces a number of flow interaction effects which must be minimized to achieve a low-drag, high-performance aircraft. These interaction effects are associated primarily with exhaust plume effects, afterbody contours, nozzle/afterbody closure, tail support boom and fairing design, control surface placement, and engine spacing, as illustrated in Fig. 1.

The engine spacing selected for the F-15 aircraft was based upon data generated during testing at the NASA Langley Research Center. The drag data presented in Fig. 2 as a function of the ratio of nozzle exit area to maximum cross-sectional area (A_{ex}/A_{max}), indicate the advantage for closely spaced engines. Figure 3 shows the effect of spacing ratio (S/D_{eng}) on the drag of the NASA configurations with values of A_{ex}/A_{max} close to those of the F-15 for cruise and afterburning conditions. For minimum drag, the desired spacing ratio clearly approaches 1.0. Structural considerations dictated the minimum engine separation distance, however, so a spacing of 1.1 was selected.

The Langley Research Center investigations were also the primary source of data for the quantitative evaluation of tail support boom interference at cruise conditions. Based on these data, two observations pertinent to nozzle/afterbody design are apparent. First, boom fairings which interfere with flow around the boattail have an adverse effect on drag. The extent to which these fairings block the flow over the nozzle

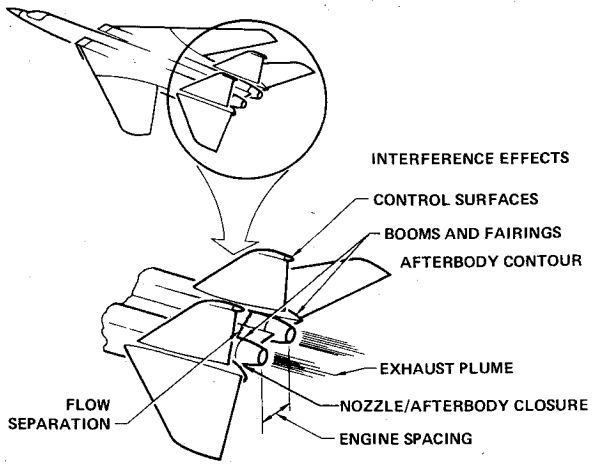

Fig. 1 Major contributors to nozzle/afterbody drag.

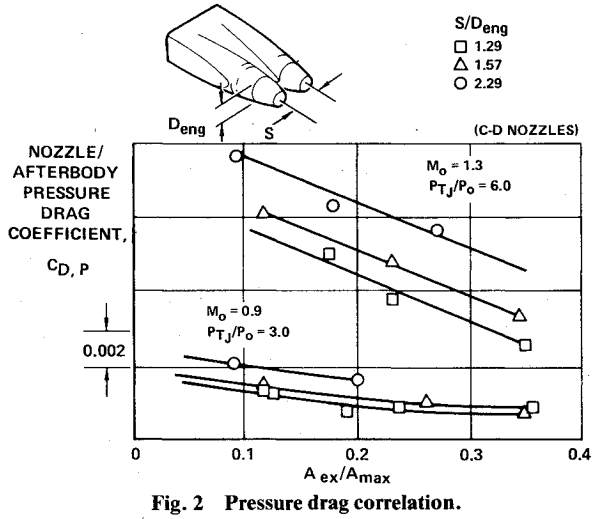

Fig. 2 Pressure drag correlation.

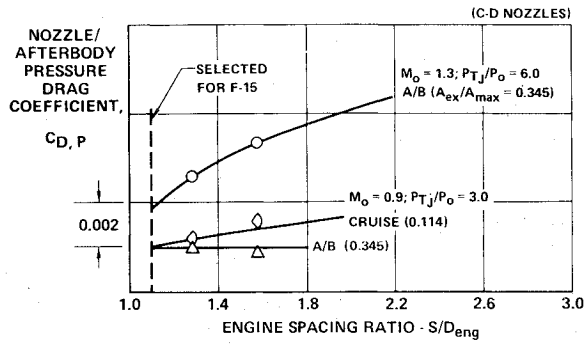

Fig. 3 Effect of engine spacing on nozzle/afterbody drag coefficient.

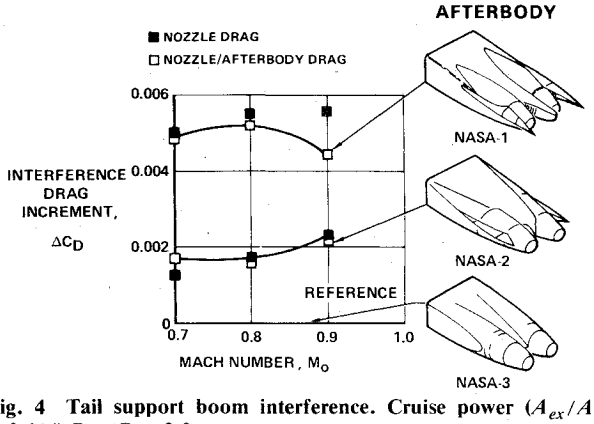

Fig. 4 Tail support boom interference. Cruise power (A_{ex}/A_{max} = 0.114) $P_{T_j}/P_0 = 3.0$.

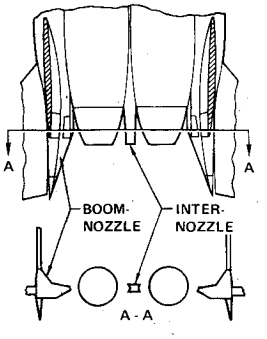

Fig. 5 Initial nozzle/afterbody configuration.

determines the level of interference drag. This is demonstrated by comparing the NASA-2 and NASA-1 interference drag increments, Fig. 4. The other pertinent observation is that the interference drag develops primarily on the nozzle. This is demonstrated in Fig. 4, where the interference increments determined using either nozzle or nozzle/afterbody drag measurements are approximately the same. Thus the importance of proper boom fairing, location and nozzle/afterbody contouring on aircraft drag becomes quite apparent.

The design of the initial F-15 nozzle/afterbody configuration, Fig. 5, was based on the Langley Research Center test results. Emphasis was placed on boom and afterbody design. The main boom structure was spaced away from the nozzle boattail as far as practical, and fairing cross-sectional areas were minimized. The area between the engine nacelles was faired from well forward on the afterbody to a 20° included-angle interfairing at the nozzle exit. This arrangement minimized blockage of flow over the nozzle boattail and reduced the region of nozzle flow separation.

The final configuration choice, of course, required numerous trade studies involving aircraft weight and performance. An example of such a trade study, involving overall body shape, is illustrated in Fig. 6. For minimum weight, the last major structural bulkhead should be located as far aft as possible. This minimizes the cantilevered structure, but imposes a relatively high afterbody slope. A more favorable approach, from a drag standpoint, involved locating the bulkhead 3 ft farther forward. This approach was selected for the F-15 because the drag reduction more than offset the weight increase.

Using these design considerations, four nozzle/afterbody configurations were fabricated for wind-tunnel testing. These configurations, Fig. 7a, were tested in the subsonic speed region with a C-D nozzle in the cruise power mode.[1] Tests were performed in the McDonnell Aircraft (MCAIR) 4-ft Polysonic Wind Tunnel in St. Louis using a 5.25% scale Jet Effects model, shown in Fig. 7b. This model was wing supported, with the complete afterbody and nozzles attached to a three-component force balance. The model simulated the F-15 forebody, except that the inlets were faired-over.

The boom interference drag levels measured on these configurations are compared with the NASA results in Fig. 8. The MCAIR configurations exhibited interference levels that were equal to, or below, those of the best NASA configuration. The MCAIR-4 configuration provided the lowest interference drag levels at high subsonic speeds, which was very important for satisfying the F-15 air superiority mission. This low drag level was attributed to wide boom spacing and termination of the boom fairing at the nozzle hinge, which permitted flow without obstruction over a large portion of the nozzle boattail. However, this design was impractical from a structural standpoint because of the thin boom-to-fuselage web. Consequently, the wide-spaced MCAIR-3 boom configuration, which provides only slightly lower performance in this critical

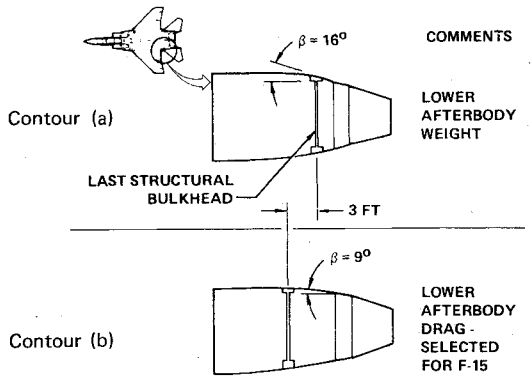

Fig. 6 Overall afterbody shape to minimize flow separation.

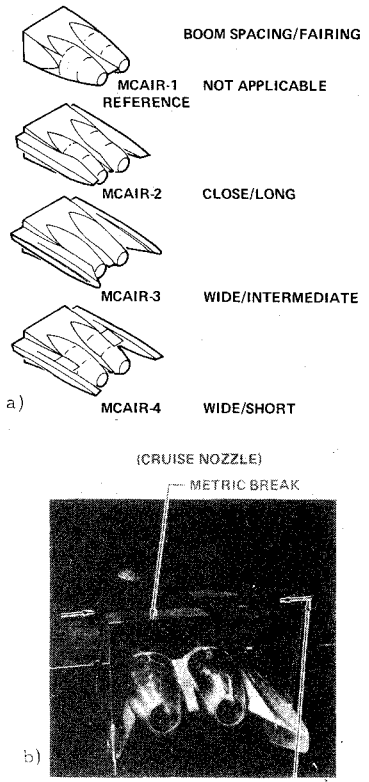

Fig. 7 Afterbody development models. a) Afterbody configurations. b) 5.25% Jet Effects Model.

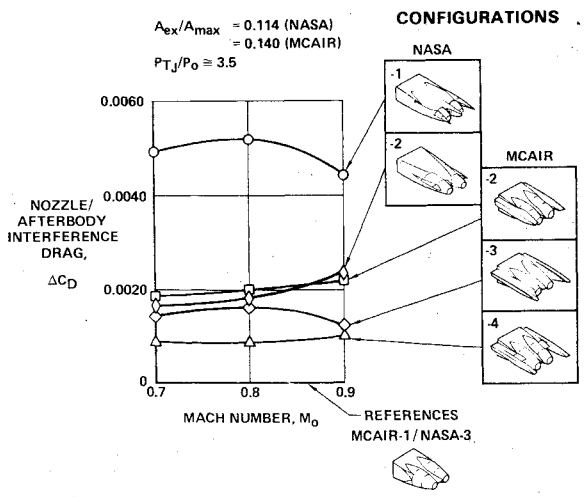

Fig. 8 Comparison of MCAIR and NASA tail support boom interference data.

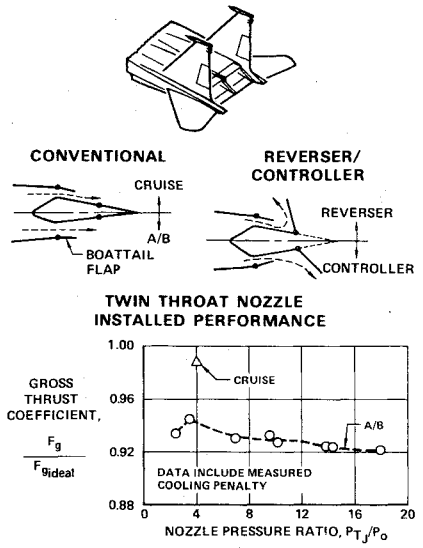

Fig. 9 Two-dimensional plug nozzle concept GE/MCAIR and P&WA/MCAIR twin throat.

speed regime, was selected as the best practical design for the axisymmetric nozzle installation.

Two-Dimensional Nozzle/Afterbody

Two-dimensional nozzles tend to integrate well with the tapering, nearly rectangular afterbody contours of aircraft with close-spaced engines. Preliminary analysis indicated that interference drag could be reduced due to improved integration and could lead to a significant performance improvement at cruise conditions. A plug nozzle design was considered the most promising 2-D configuration, primarily because it provided lower boattail angles than 2-D convergent or convergent-divergent designs.

An extensive development program to explore the feasibility of utilizing such a design was undertaken in conjunction with both General Electric (GE) and Pratt & Whitney Aircraft (P&WA). In the concept selected for evaluation, Fig. 9, a double wedge is mounted horizontally across the exhaust duct, thereby providing "twin-throats" for each nozzle. Another attractive feature of this design is its simple adaptability to thrust control or reversal, although this was not an F-15 requirement.

The installed performance of the Twin-Throat nozzle, also shown of Fig. 9, was based upon wind-tunnel data with adjustments being made for plug cooling penalties. The cruise performance is somewhat higher than that of the afterburning nozzle because of beneficial external flow effects and reduced cooling requirements. Recompression of the external flow results in a favorable pressure on the nozzle plug. To achieve this advantage however, the nozzle must be integrated to avoid flow separation on the boattail. The performance of the afterburning nozzle is not sensitive to external flow because the last exit expansion wave does not intersect the plug.

The cooling airflow requirements were predicted using empirical/analytical procedures and verified during hot gas testing. General Electric utilized a 25% scale hot flow model in their verification testing, while P&WA installed a full-scale plug behind an afterburning J-58 engine. Detailed weight estimates were based on these data.

Nearly 200 different configurations were tested with no external flow to determine the best internal geometry for conventional, modulated, and reverse thrust applications. Dry power reverse thrust levels of $F_{g_{rev}}/F_{g_{ideal}} = 0.6$ were demonstrated without flow reduction. Subsequent wind-tunnel testing of the thrust controllers demonstrated a 70% reduction in gross thrust at Mach .9.

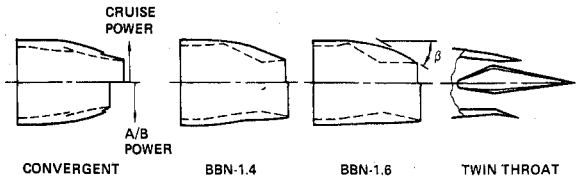

CONFIGURATION			CRUISE POWER MACH NO. = 0.9			MAX AFTERBURNING MACH NO. = 2.2		
ENGINE NOZZLE	NOZZLE WT (LB)	$\frac{A_{ex}}{A_t}$ (a)	β (DEG)	ΔC_D (c)	$\frac{F_g}{F_{g\,ideal}}$	β (DEG)	ΔC_D (c)	$\frac{F_g}{F_{g\,ideal}}$
REF CONVERGENT	357	1.00	19.4	0.0025	0.9730	11.9	0.0007	0.878
BBN (b) - 1.4	310	1.41	27.1	0.0025	0.9833	7.2	0.0003	0.948
BBN - 1.6	345	1.61	24.5	0.0026	0.9840	7.4	0.0003	0.957
TWIN THROAT	640	1.50	16.1	0.0005	0.9890	−6.6	0.0002	0.926

(a) Maximum Internal Area Ratio
(b) P&WA Balanced Beam Nozzle (BBN)
(c) Drag Relative to Cylindrical A/B Nozzle at $P_{ex} = P_o$

Fig. 10 Nozzle trade study data summary.

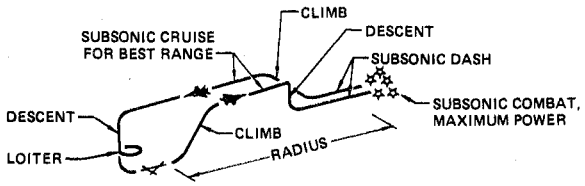

ENGINE NOZZLE	(a) ΔTOGW (LB)	(b) MAINTAINABILITY (MMH/FH)	TECHNICAL RISK	SPECIFIC EXCESS POWER INCREMENT, $\Delta P_s/P_{s_{REQ}}$ (c) SUBSONIC EM POINT MIL POWER (%)	SUBSONIC EM POINT MAX POWER (%)	SUPERSONIC EM POINT MAX POWER (%)	RANK
REF CONVERGENT	0	--	LOW	48	63.0	−39.7	4
BBN - 1.4	−521	0.0450	LOW	57	69.5	−21.0	2
BBN - 1.6	−413	0.0450	LOW	56	65.0	+55.0	1
TWIN THROAT	+410	0.0340	HIGH	65	36.5	−14.6	3

(a) Compared to Reference Convergent Nozzle
(b) Maintenance Manhours per Flight Hour
(c) Energy Maneuverability (EM) Point Requirement ($P_{s_{Req}}$):
$\Delta P_s = P_{s_{Candidate}} - P_{s_{Req}}$

Fig. 11 Nozzle trade study results. Constant air superiority mission performance P&WA engine.

Configuration Selection

The final nozzle/afterbody design selection was based on extensive aircraft performance trade studies using the test data reviewed above. Six axisymmetric C-D nozzle configurations, representing designs from both engine companies, and the MCAIR 2-D Twin-Throat nozzle design were considered. The characteristics of the P&WA nozzles, as well as the Twin-Throat and the baseline nozzle, are presented in Fig. 10. The weight and internal performance for these axisymmetric nozzles were furnished by P&WA, while the Twin-Throat nozzle estimates were based upon the results of the joint MCAIR/engine company test programs. Estimates of installed drag were made using available data to augment the previously described axisymmetric and 2-D plug nozzle test data.

The factors considered in the trade study were installed performance, weight, development status (or technical risk), and maintainability. The aircraft performance and takeoff gross weight (TOGW) for each candidate configuration were obtained using automated performance prediction techniques. Each aircraft was sized to provide a specified mission range and specific excess power (P_s) was then calculated at several maneuvering points. The trade study results are summarized in Fig. 11.

The high area ratio P&WA 1.6 nozzle was selected for the F-15 because it satisfied the maneuvering performance requirements and minimized the risk at the lowest weight. The selected nozzle/afterbody configuration was characterized by close-spaced, axisymmetric C-D nozzles installed in a carefully contoured afterbody with wide-spaced tail support booms.

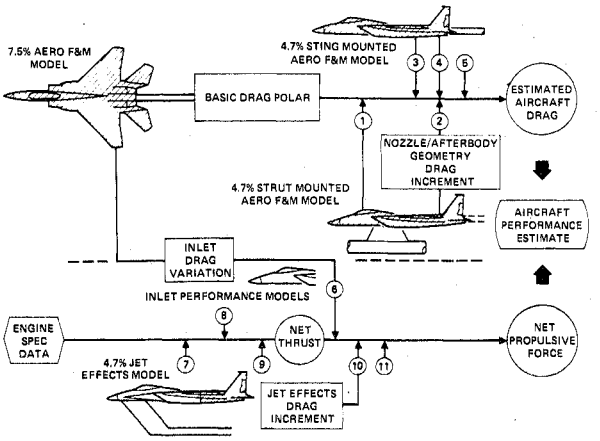

Fig. 12 F-15 thrust drag accounting system: 1) sting interference corrections; 2) nozzle/afterbody geometry (cruise to *A /B)*; 3) high angle-of-attack status; 4) external store drag; 5) roughness and Reynolds number correction; 6) inlet drag force correction to operg mass flow ratio; 7) internal nozzle performance; 8) inlet flowfield, distortion, recovery; 9) power extraction, compressor bleed; 10) nozzle/afterbody drag correction from flow through to operating jet pressure ratio; 11) inlet bleed, bypass, compartment ventilation, ECS, and leakage drags.

The Twin-Throat nozzle was eliminated on the F-15 because of a significant aircraft TOGW penalty and high technical risk. The weight penalty resulted, in part, from the performance loss associated with plug cooling requirements. The potential of 2-D nozzles, especially in the area of improved nozzle/airframe integration, was obvious however. This development work verified the validity of the Twin-Throat nozzle concept for improving installed thrust-minus-drag performance, although work in the weight and cooling areas remains to be accomplished.

Nozzle/Afterbody Refinement and Performance Prediction

Additional design studies and wind-tunnel tests were conducted to refine the nozzle/afterbody design. The resulting data were used in conjunction with other elements in the F-15 thrust/drag accounting system to estimate full-scale flight performance. Although complete flight test performance results are not available for comparison, limited comparisons of model and full-scale surface static pressure distributions have been made.

Thrust/Drag Accounting

To insure the best possible results in predicting full-scale performance, special emphasis was placed on defining a thrust/drag accounting system which permits accurate assessment of the aircraft and propulsion system performance elements. This approach influenced the selection of wind-tunnel models and test reference conditions.

The final F-15 thrust/drag accounting system and the related performance models are shown schematically in Fig. 12. A strut supported Aerodynamic Force and Moment model (Aero F&M) and a Jet Effects model, Fig. 13, were used to obtain the effects on performance of nozzle/afterbody geometry and jet effects, respectively.

The Aero F&M model was fully metric, with inlet mass flow controlled by simple convergent nozzle chokes. Aircraft external lines, including cruise and afterburning nozzle contours, were simulated on this model. The Jet Effects model was partially metric and included control surfaces and faired-over inlets. High-pressure air was routed through the strut to permit simulation of the engine exhaust plume. The strut had

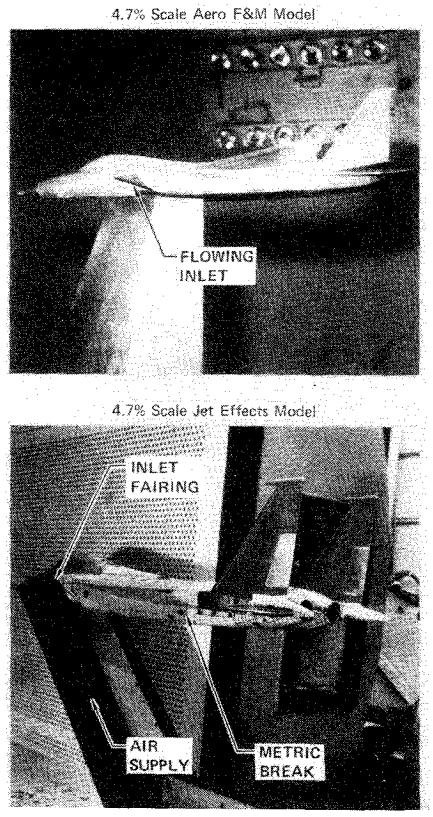

Fig. 13 F-15 wind-tunnel models for nozzle/afterbody refinement and performance prediction.

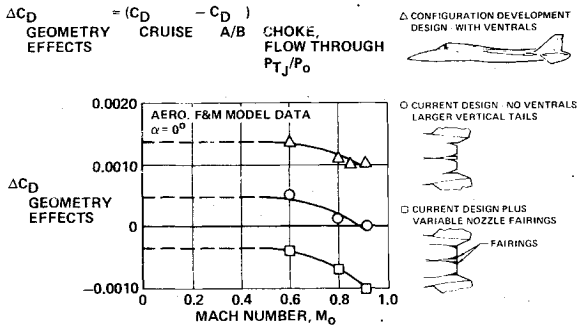

Fig. 14 Cruise nozzle/afterbody geometry increments.

to be somewhat thicker than on the Aero F&M model to incorporate the air lines. This model was used to obtain the corrections for differences in jet pressure ratio and nozzle internal geometry between the Aero F&M model and the aircraft.

A study was performed to determine how accurately the effects of nozzle/afterbody geometry changes on performance could be determined using a Jet Effects model. These studies indicated bias errors due to: 1) support system interference, 2) inlet fairing effects, and 3) metric-to-nonmetric splitline locations. The errors were highest at Mach 0.9 and for geometry changes near the splitline. Although it was concluded that preliminary configuration development could be accomplished using a Jet Effects model, the strut supported Aero F&M model was used for more accurate evaluation of geometry effects during refinement and performance prediction testing.

Configuration Refinement and Performance Prediction

Configuration refinement and performance testing included investigations of the effects of nozzle fairing geometry, nozzle closure, nozzle pressure ratio, vertical tail and ventral

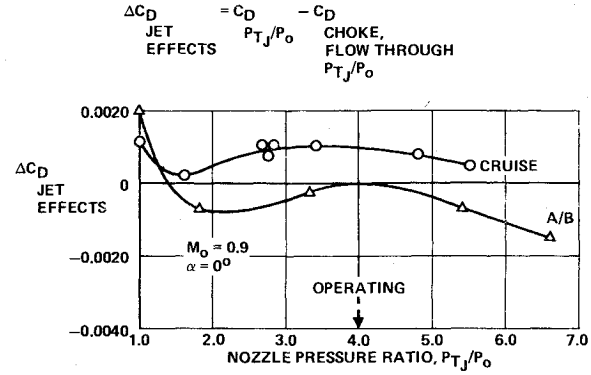

Fig. 15 Nozzle/afterbody jet effects increments.

location, and base bleed. The Aero F&M and Jet Effects models were utilized, with testing in both the MCAIR Polysonic Wind Tunnel and the NASA-Langley 16-ft transonic tunnel. The Mach numbers ranged from 0.6-2.5 at angles of attack from −3°-15°. Forces and moments were measured on both models. Surface static pressures were also measured on the Jet Effects model during tests at the Langley Research Center.

The results of the configuration refinement tests are presented in Fig. 14 in terms of the nozzle/afterbody geometry drag increment. These data were measured on the strut supported Aero F&M model. The removal of ventral fins, which was offset by a 12% increase in vertical tail size, produced a reduction in drag coefficient of 0.0011 at Mach 0.9. This change was incorporated into the final aircraft design.

The influence of the exhaust plume on nozzle/afterbody drag at Mach 0.9 is shown in Fig. 15. At cruise operating conditons, the exhaust plume increases the drag coefficient by 0.0009. There is no drag change at afterburning conditions for this Mach number.

The total nozzle/afterbody drag increments used in the projection of F-15 flight performance are shown in Fig. 16. These increments represent the drag correction to the Aero F&M model, with afterburning choke nozzles operating at flow-through pressure ratio. In the subsonic regime, the drag correction ranges from zero for the afterburning nozzles to $\Delta C_D = 0.0018$ for the cruise nozzle. Supersonically, the correction for afterburning conditions reduces the drag, ranging from $\Delta C_D = -0.0015$-0.0040, depending upon Mach number. This reduction is caused by the favorable interaction of the expanding jet plume with the afterbody flowfield.

Model to Flight Comparisons

Flight-test data acquisition has been concentrated on obtaining total system performance. Model-to-flight comparisons to date have typically agreed within the accuracy of the data. More complete comparisons, in terms of thrust and total aircraft drag, will become available when analysis of instrumented engine data is completed. However, nozzle/afterbody static pressures, measured on both the Jet Effects model and flight test vehicle, are available for comparison.

Model and flight pressure distributions, measured on the afterbody and cruise nozzles, are presented in Figs. 17 and 18. The most valid comparisons are on the upper surfaces of the nozzle and afterbody, because the model data were obtained on a configuration which incorporated ventral fins. For these locations, the flight data exhibits higher pressures on the afterbody and forward portion of the nozzle boattail. Aft of FS 795, the model and flight data tend to be relatively constant, which is indicative of flow separation. The higher flight-test pressures on the lower surface of the nozzle, forward of FS 795, can probably be atrributed to the absence of ventral fins on the full-scale aircraft.

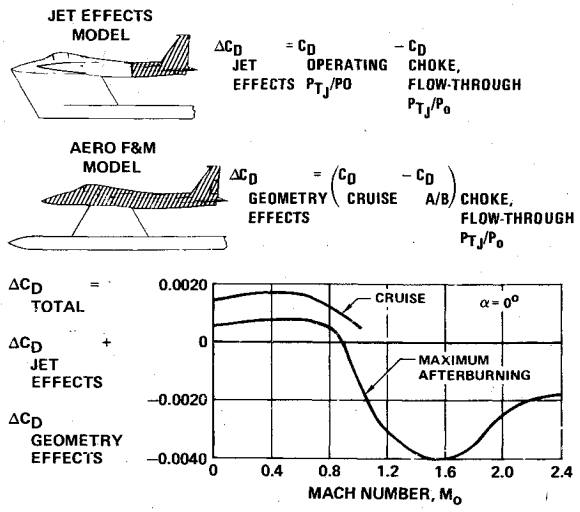

Fig. 16 Total F-15 nozzle/afterbody drag increments.

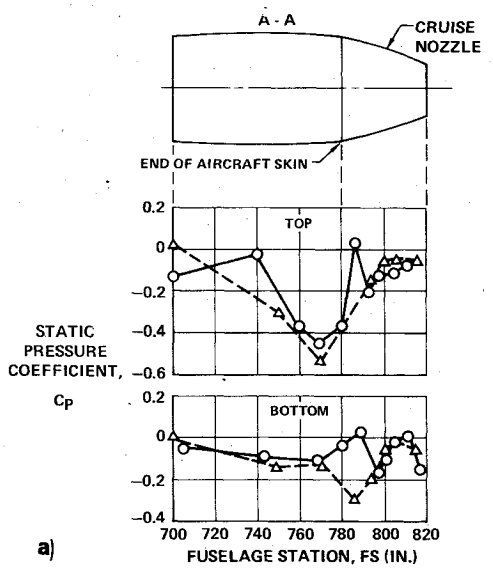

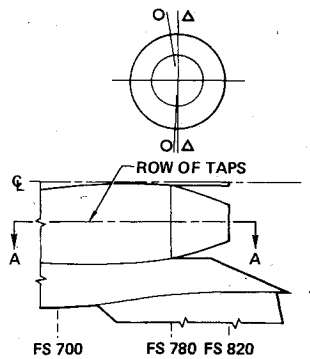

	○ FLIGHT TEST	△ MODEL TEST
M_o	0.877	0.853
α (DEG)	5.4	6.0
ALT (FT)	10,800	–
P_{T_J}/P_o	2.96	3.14
R_e (1)	2.7×10^8	1.2×10^7
VENTRALS	OFF	ON

b) (1) Based on Total Fuselage Length

Fig. 17 Model to flight comparison of F-15 nozzle/afterbody pressure coefficients. a)Comparison. b) Legend.

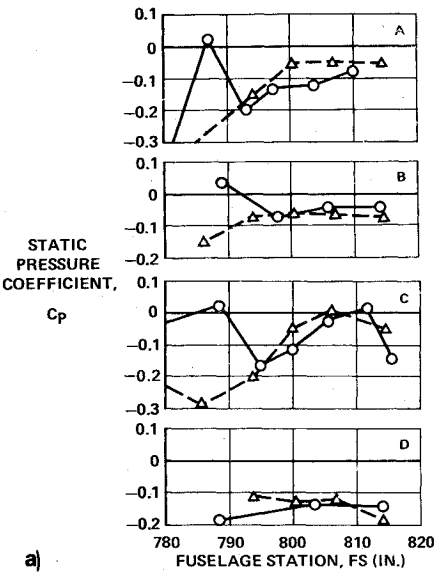

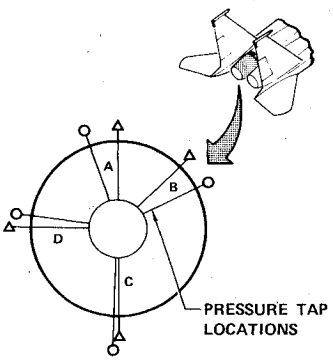

	○ FLIGHT TEST	△ MODEL TEST
M_o	0.877	0.853
α (DEG)	5.4	6.0
ALT (FT)	10,800	–
P_{T_J}/P_o	2.96	3.14
R_e (1)	2.7×10^8	1.2×10^7
VENTRALS	OFF	ON

b) (1) Based on Total Fuselage Length

Fig. 18 Model to flight comparison of F-15 nozzle pressure coefficients. a) Comparison. b) Legend.

	□ FLIGHT TEST
P_{T_J}/P_o	1.8 - 3.7
ALT (FT)	5 - 20k
α (DEG)	1.1 - 5.4
R_e (1)	$1.4 \rightarrow 3.2 \times 10^8$

(1) Based on Total Fuselage Length

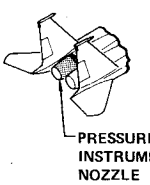

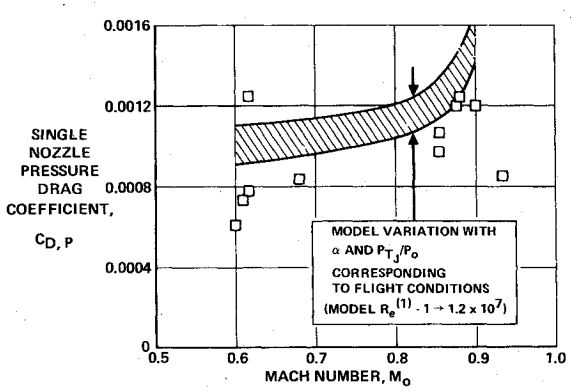

Fig. 19 Comparison of F-15 model and full scale nozzle drag, cruise nozzle.

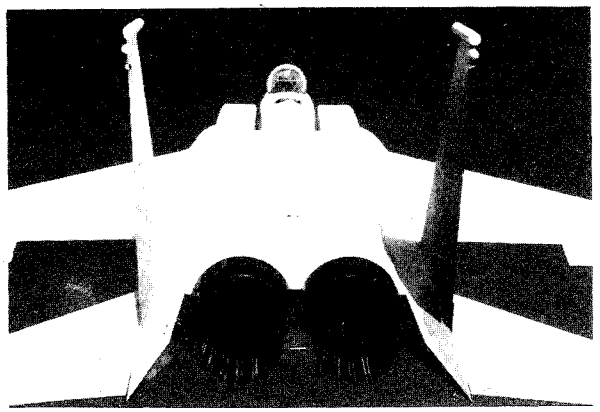

Fig. 20 F-15 nozzle/afterbody.

The nozzle boattail pressures were integrated from the end of the aircraft surface, FS 780, to the nozzle exit to permit convenient comparison of the model and flight nozzle drag data over a range of Mach numbers, Fig. 19. The model drag is represented by a band which brackets the variation due to flight angle-of-attack and pressure ratio. The flight data are considered less accurate, since only 18 pressures were measured, compared to 36 on the model. The limited flight-test data are slightly lower than the model data, but exhibit the same drag rise characteristics. Based on these limited comparisons, it is concluded that the F-15 test techniques led to relatively accurate, but perhaps conservative subsonic performance predictions.

Conclusions

A well-integrated nozzle/afterbody configuration was selected for the F-15, following an extensive analytical and experimental development program. This configuration, illustrated in Fig. 20, is characterized by close-spaced axisymmetric C-D nozzles, wide-spaced tail support booms, and a carefully contoured afterbody. It was selected over a lower drag 2-D Twin-Throat nozzle installation because of weight and development status considerations.

Design of the axisymmetric nozzle installation was based on MCAIR and NASA model data that showed: 1) minimum engine spacing provides the lowest drag in the transonic speed regimes; 2) lowest interference drag levels result from wide-boom spacing at transonic speeds; 3) low interference drag can be obtained by careful design of the afterbody contours and proper contouring of the booms; and 4) removal of ventral fins can reduce cruise drag by $\Delta C_D = 0.0011$.

The total nozzle/afterbody drag corrections to the basic aircraft polars, to account for nozzle geometry and jet effects, are small at subsonic conditions. At Mach 0.9, the cruise correction increases the drag by $\Delta C_D = 0.0009$, while the afterburning correction is zero. However, at supersonic maximum afterburning conditions, the correction decreases the basic drag coefficient as much as $\Delta C_D = 0.0040$ (at Mach 1.6).

Limited comparisons of nozzle/afterbody pressures at subsonic speeds indicate higher pressures on the full-scale afterbody and forward portion of the nozzle boattail. Comparisons of integrated nozzle boattail pressures indicate that the flight-test drags are slightly lower, but the drag rise characteristics are similar to those obtained on the model.

Reference

[1] Eigenmann, M.F. and Hiley, P.E., "Analysis of Wind Tunnel Data on a 5.25% Scale Jet Effects Model in the McDonnell Polysonic Wind Tunnel-PSWT 233," McDonnell Douglas Co., St. Louis, Mo., MDC Rept. A3036, Oct. 1969.